Joule

CellPress

Article

4.0 V Aqueous Li-Ion Batteries

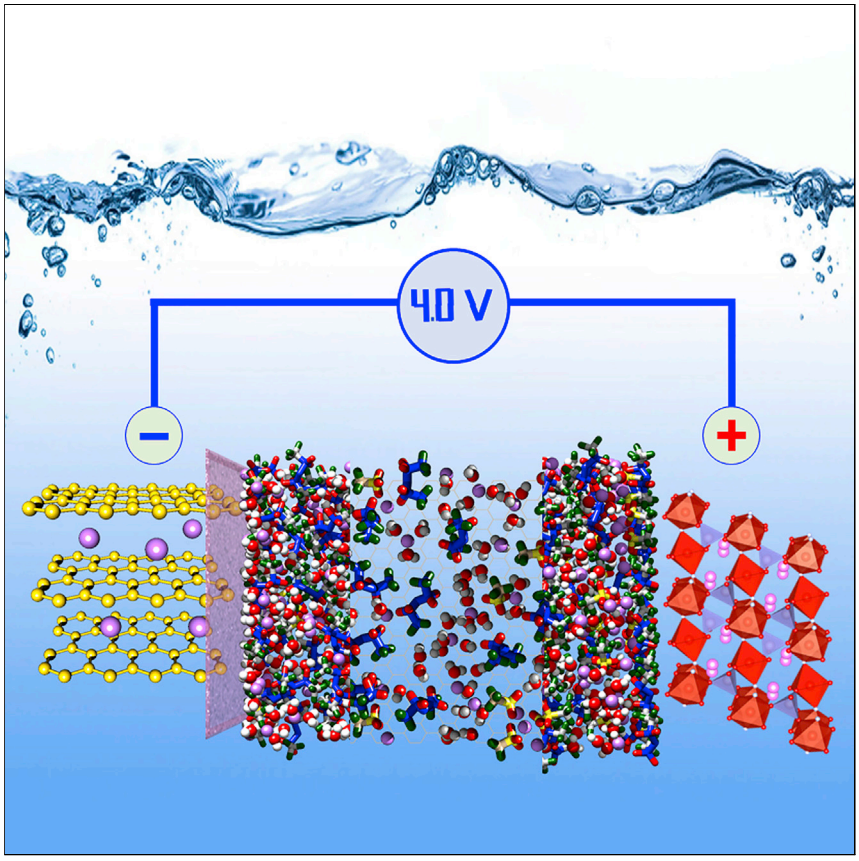

4.0 V aqueous LIBs of both high energy density and high safety are made possible by a new interphase formed from an "inhomogeneous additive" approach that effectively stabilizes graphite or lithium-metal anode materials.

Chongyin Yang, Ji Chen, Tingting Qing, ..., Nico Eidson, Chunsheng Wang, Kang Xu

cswang@umd.edu (C.W.)
conrad.k.xu.civ@mail.mil (K.X.)

HIGHLIGHTS

A new aqueous solid-electrolyte-interphase (SEI) is engineered

This SEI stabilized graphite and lithium-metal anodes in aqueous electrolyte

4.0 V class aqueous LIBs with high energy density and safety are enabled

Yang et al., Joule *1*, 122–132
September 6, 2017 Published by Elsevier Inc.
http://dx.doi.org/10.1016/j.joule.2017.08.009

Joule

CellPress

Article

4.0 V Aqueous Li-Ion Batteries

Chongyin Yang,[1] Ji Chen,[1] Tingting Qing,[1] Xiulin Fan,[1] Wei Sun,[1] Arthur von Cresce,[2] Michael S. Ding,[2] Oleg Borodin,[2] Jenel Vatamanu,[2] Marshall A. Schroeder,[1] Nico Eidson,[1,2] Chunsheng Wang,[1,3,*] and Kang Xu[2,4,5,*]

SUMMARY

Although recent efforts have expanded the stability window of aqueous electrolytes from 1.23 V to >3 V, intrinsically safe aqueous batteries still deliver lower energy densities (200 Wh/kg) compared with state-of-the-art Li-ion batteries (~400 Wh/kg). The essential origin for this gap comes from their cathodic stability limit, excluding the use of the most ideal anode materials (graphite, Li metal). Here, we resolved this "cathodic challenge" by adopting an "inhomogeneous additive" approach, in which a fluorinated additive immiscible with aqueous electrolyte can be applied on anode surfaces as an interphase precursor coating. The strong hydrophobicity of the precursor minimizes the competitive water reduction during interphase formation, while its own reductive decomposition forms a unique composite interphase consisting of both organic and inorganic fluorides. Such effective protection allows these high-capacity/low-potential anode materials to couple with different cathode materials, leading to 4.0 V aqueous Li-ion batteries with high efficiency and reversibility.

INTRODUCTION

Since their birth almost three decades ago, lithium-ion batteries (LIBs) have reshaped our life with their omnipresence in portable electronics. While being gradually adopted into power trains of electric vehicles and grid storage, large-format LIBs (>30 Ah) are more and more rigorously scrutinized for their safety, as their rare but high-profile fire/explosion accidents and subsequent recalls have cast increasing doubt over their large-scale applications. Upon close examination, the fundamental cause of those safety hazards can be identified as the undesired combination of high-energy electrodes and flammable non-aqueous electrolytes in LIB. The latter carry the intrinsic disadvantages of being flammable, toxic, and highly sensitive to ambient atmosphere.[1,2] Clearly, resolution of LIB safety concerns on a materials level requires the removal of at least one factor from the equation: the high-energy electrode as the main energy source or the non-aqueous electrolyte solvents (carbonate esters) as fuel in the chemical combustion following accidental thermal runaway.

Water emerges as a natural replacement for the flammable non-aqueous solvents, because it is not only non-flammable but also an excellent solvent as characterized by high dipole moment (1.8546 Debye), high acceptor and donor numbers (AN = 54.8, DN = 18) as well as high dielectric constant (ε = 78 at 25°C).[3] However, water offers a rather narrow electrochemical stability window, which is ~1.23 V under thermodynamic equilibria. At pH 7.0, its cathodic and anodic limits are located at 2.62 V and 3.85 V versus Li, respectively, while most LIB chemistries situate far beyond these limits (e.g., Li metal, 0.0 V; graphite, 0.10 V; silicon, 0.30 V; $LiMnO_2$, 4.10 V; $LiNi_{1/3}Mn_{1/3}Co_{1/3}O_2$, 4.20 V; and $LiNi_{0.5}Mn_{1.5}O_4$, 4.60 V).[4] Those few that do fit in

Context & Scale

Constrained by the narrow electrochemical stability window of water (1.23 V under thermodynamic equilibria), aqueous batteries have always been considered subpar to their non-aqueous counterparts in terms of energy density, although the latter bear the intrinsic disadvantages of being flammable, toxic, and sensitive to ambient atmosphere. Here, we report a unique strategy of stabilizing lithium metal or graphite in an aqueous electrolyte, so that a series of 4 V class aqueous Li-ion chemistries could be enabled. Such aqueous Li-ion batteries, expected to offer energy densities approaching those of non-aqueous Li-ion batteries, but without the safety concern of the latter, represent a significant advance on the fundamental level of battery materials.

this narrow electrochemical stability window (such as $LiTi_2(PO_4)_3$, 2.70 V; TiP_2O_7, 2.90 V; VO_2, 2.70 V; and $LiFePO_4$, 3.50 V) can only assemble aqueous batteries with cell voltages below 1.50 V and energy densities below 70 Wh/kg, along with significantly compromised cycling stabilities.[5]

More recently, ground-breaking efforts were made to expand this stability window of water by transplanting the solid-electrolyte-interphase (SEI) concept from non-aqueous electrolytes, so that the surfaces of those electrodes would be kinetically protected while operating beyond the above limits.[6,7] That work had led to a new class of aqueous electrolytes, as represented by the so-called "water-in-salt" electrolytes (WiSE) named after their high salt concentration. WiSE and its many variations can form an *ad hoc* SEI on the anode during the initial charging, offering an electrochemical stability window of >3.0 V and enabling diversified aqueous battery chemistries with cell voltages and energy densities as high as 3.0 V and 200 Wh/kg, respectively.[6–10] However, a significant gap still exists between these improved energy densities and what the state-of-the-art LIB can offer (400 Wh/kg). This gap mainly originates from the awkward positioning of the cathodic stability limits of these aqueous electrolytes, which, without exception, all situate between 1.7 and 1.9 V versus Li, thus excluding the most energy-dense anode materials such as silicon, graphite, and Li metal. On the other hand, most cathode materials are comfortably accommodated by the anodic stability limits (~4.90 V) of WiSE and its variations. By judicious selection of current collectors, even the so-called 5.0 V class cathode $LiNi_{0.5}Mn_{1.5}O_4$ could be partially supported.[7]

RESULTS

The above uneven positioning of cathodic and anodic limits in super-concentrated aqueous electrolyte stems from the preferential distribution of water molecules and salt anions at the inner-Helmholtz interface of the electrode as potential is applied. Snapshots from molecular dynamics (MD) simulations (Figure 1) reveal such unsymmetrical rearrangement of "water-in-bisalt" electrolyte (WiBS), i.e., aqueous solution of 21 M lithium bis(trifluoromethane)sulfonyl imide (LiTFSI) + 7 M lithiumtrifluoromethane sulfolate (LiOTF),[11] when the electrode is cathodically polarized. At 2.5 V versus Li, LiTFSI and LiOTF dominate the inner-Helmholtz layer, while water is almost excluded from direct contact with the graphite surface (Figure 1A). Such an interfacial chemical composition favors the formation of an SEI mainly contributed by the reductive decomposition of these fluorinated salt anions. Anode materials with moderate lithiation or sodiation potentials (such as Mo_6S_8 or $NaTi_2(PO_4)_3$) would fall into this category,[6,10] where LiF- or NaF-based SEIs have been observed. However, as electrode potential is further polarized to 0.50 V and below, these anions experience increasing expulsion from a surface now negatively charged, and a large fraction of water molecules start to adsorb with hydrogens pointing toward the surface, making them readily available for the hydrogen evolution reaction that becomes energetically favorable at this potential (Figure 1B). Such interfacial structure disfavors salt anion decomposition, and the SEI formation would be severely disrupted by the hydrogen evolution. Thus, anode materials with lithiation potentials below 0.5 V (such as silicon, graphite, and lithium metal) would face severe "cathodic challenge" that cannot be simply resolved by increasing salt concentrations.

Hence, in order to render an aqueous LIB competitive in energy density against the state-of-the-art LIB, one must resolve this "cathodic challenge" of a gap of more than 1.5 V via additional protection. An effective strategy would be the

[1]Department of Chemical and Biomolecular Engineering, University of Maryland, College Park, MD 20740, USA

[2]Electrochemistry Branch, Sensor and Electron Devices Directorate, Power and Energy Division, US Army Research Laboratory, Adelphi, MD 20783, USA

[3]Senior author

[4]Senior author

[5]Lead Contact

*Correspondence: cswang@umd.edu (C.W.), conrad.k.xu.civ@mail.mil (K.X.)

http://dx.doi.org/10.1016/j.joule.2017.08.009

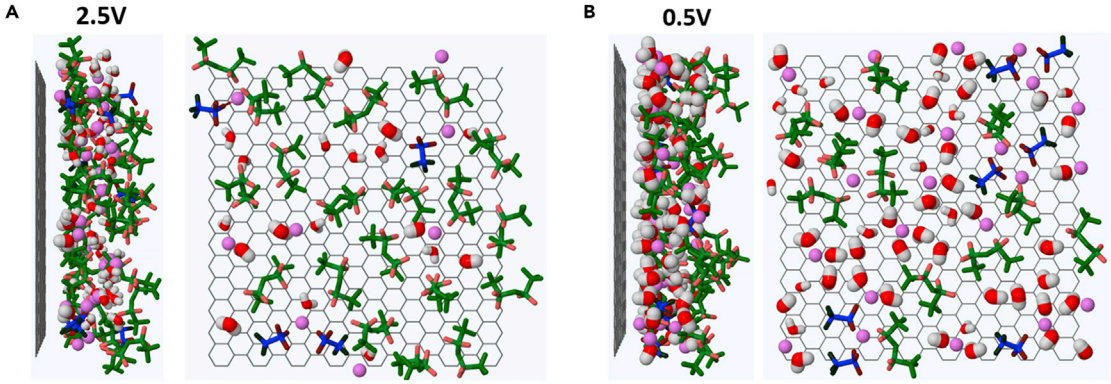

Figure 1. Representative MD simulations

For a Figure360 author presentation of Figure 1, see http://dx.doi.org/10.1016/j.joule.2017.08.009#mmc6.

(A and B) Snapshots of inner-Helmholtz interfacial regions of the anode surface in WiBS (21 M LiTFSI + 7 M LiOTF in water) at (A) 2.5 V and (B) 0.5 V versus Li, respectively. Water molecules adsorbed or closer than 4 Å to the surface are magnified, while water molecules further removed from the surface are shown as slightly reduced in the picture.

minimization of water molecules at the anode surface before the SEI forms. In this work, we approached this challenge with an "inhomogeneous SEI additive" strategy. Such an additive is immiscible with WiSE but can be applied as a thin coating in the form of gel on the surface of either graphite or Li metal. Due to its strongly hydrophobic nature, it expels water molecules from the anode surface, thus minimizing the competing water decomposition during the initial forming cycle, and creating a favorable environment for the formation of a conformal and dense interphase. Upon lithiation of the anode, this inhomogeneous additive decomposes into an SEI rich in both inorganic LiF and organic C-F species, which for the first time enables the reversible cycling of these anode materials in aqueous electrolytes.

Apparently, the *ad hoc* interphases originating alone from WiSE or its improved derivatives can only protect the anode materials that operate at relatively high potentials such as Mo_6S_8, $Li_4Ti_5O_{12}$, anatase TiO_2, or $NaTi_2(PO_4)_3$.[6–10] Earlier on we had found that, although graphite or Li metal cannot be stably cycled in WiSE, its reactivity toward these anode materials has been extremely low due to the significantly reduced water activity at such high salt concentrations (Figure S1 and Movie S1). Such reactivity is even further reduced when an improved WiSE is "solidified" with the formation of hydrogel (gel-WiSE; Figure S2 and Movie S2) using either polyvinyl alcohol (PVA) or polyethylene oxide (PEO).[9] However, any attempt to cycle graphite or Li metal in these gel-WiSE still failed, because of the above-mentioned "cathodic challenge," which creates a gap of more than 1.5 V between the cathodic limit of WiSE (~1.7 V versus Li) and the working potentials of either graphite (~0.1 V versus Li) or Li metal (0 V versus Li). Water decomposition driven by the interfacial structure as shown in Figure 1B cannot be kinetically suppressed by an *ad hoc* SEI, because its formation from the reduction of TFSI or OTF is now disfavored and has to compete with hydrogen evolution. Employing super-concentration to fight the "cathodic challenge" is neither realistic nor effective because of the concerns over viscosity, cost, and solubility limits. In fact, WiBS[11] and hydrate melt[7] (both with ~28 M salt) have nearly reached their saturation limits, but the widening of the electrochemical stability window is rather incremental compared with the original WiSE, as dictated by the preferential exclusion of salt anions near the inner-Helmholtz region (Figure 1B). Additional assistance is thus needed to counter such an undesired preference, such as an interphase-forming additive.[2,12]

In non-aqueous electrolytes, interphase-forming additives were customarily employed to strengthen the chemical durability of these SEIs, and their selection criteria usually center around their capability of being preferentially reduced before bulk electrolyte components.[12] However, application of the additive practice to aqueous electrolytes has to be subject to a number of new constraints. First, as the precursor of an additional interphase, the additive must be chemically stable against WiSE or gel-WiSE; Second, it must be electrochemically unstable so that it can release the interphase ingredient on demand; Third and most importantly, the precursor should effectively exclude water molecules from the surface of these anode materials so that the interfacial favor on hydrogen evolution would be effectively countered. In other words, such an additive should be ideally phase separated from WiSE before its decomposition, which significantly differs from conventional additives that are well miscible with the bulk non-aqueous electrolytes. Finally, considering that the aqueous SEIs successfully formed so far for either Li-ion or Na-ion chemistries mainly consist of fluoride salts (LiF or NaF) as a consequence of TFSI reduction,[6,9,10] ingredients that are most likely insoluble in aqueous media, the interphase additive should contain a rich fluorine source. The combination of the above constraints rules out most additives familiar to non-aqueous electrolytes, such as sultones, phosphates, borates, or any compounds with labile fluorine bonds, because they are either susceptible to hydrolysis, or form products that are soluble in water, or are miscible with WiSE so that the initial formation chemistry of the additional interphase has to compete with hydrogen evolution, resulting in low efficiency and a highly porous interphase that will poorly adhere to the anode surface.

After a lengthy screening process, we eventually selected a highly fluorinated ether (HFE) as such an "inhomogeneous additive". 1,1,2,2-Tetrafluoroethyl-2′,2′,2′-trifluoroethyl ether (Figure S3A) is completely immiscible with WiBS, a variation of WiSE[11] (Figure S3B). Although ethereal compounds in general are considered more resilient against reductive decomposition, the energy level of the lowest occupied molecular orbital for HFE should have been significantly brought down by its high degree of fluorination, thus HFE could satisfy the basic requirement for an electrolyte additive: to electrochemically decompose (see Figure S3C) and to provide the interphase building blocks. Upon mixing with 0.5 M LiTFSI, HFE forms a translucent gel in the presence of 10 wt % polyethylene oxide at 70°C (denoted as LiTFSI-HFE gel hereafter; Figure S4), which remains phase separated from either WiSE or gel-WiSE (Figure S5). Due to the sluggish dissolution process of LiTFSI in HFE, ca. 5% dimethyl carbonate (DMC) was sometimes optionally added to assist the gel formation. Most of the DMC (boiling temperature 90°C) was then evaporated, leaving the translucent gel, which is immiscible with WiSE. Fourier-transform infrared spectroscopy cannot detect any residual DMC in this LiTFSI-HFE gel (on the other hand, LiTFSI solution in neat DMC mixes well with either WiSE or WiBS). The extremely hydrophobic nature of LiTFSI-HFE gel is well demonstrated by its complete immiscibility with WiSE or WiBS as well as its moisture content of ~35 ppm at equilibrium after exposure to WiSE for 50 hr (Figure S6). Such a low moisture level is acceptable even by the standard of non-aqueous electrolytes, and should not interfere with the effective interphase formation reaction on graphite surfaces and the reversible Li^+-intercalation/de-intercalation. It also displays complete inertness toward Li metal, as does WiSE (Figure S7).

Pre-coating a graphite electrode or a Li-metal foil with a thin layer of LiTFSI-HFE gel enables the stable cycling of these anode materials in gel-WiSE without apparent hydrogen evolution. Figure 2A displays cyclic voltammetry (CV) performed on such a protected graphite electrode in gel-WiBS. A minor peak appears in the first

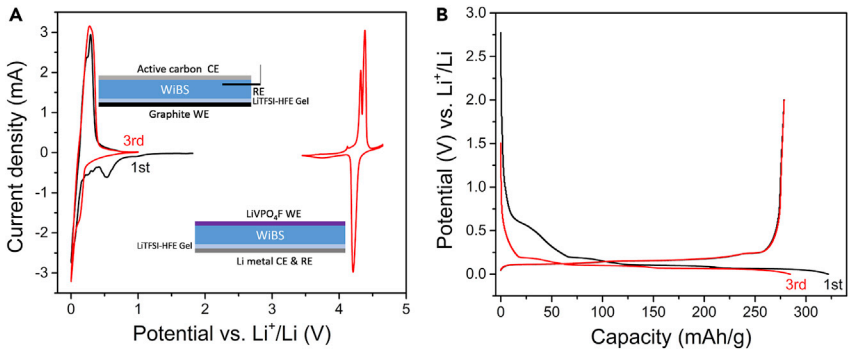

Figure 2. 4.0 V Stability Window and Stabilization of Graphite Lithiation in Aqueous Electrolyte

(A) Cyclic voltammograms of a graphite anode pre-coated with LiTFSI-HFE gel. The CV is conducted in gel-WiBS (working electrode, WE) with an Ag/AgCl reference electrode (RE) and active carbon counter electrode (CE). The potential has been converted to a Li/Li^+ reference for visual convenience. Also displayed in the figure on anodic side is the CV of a $LiVPO_4F$ cathode in gel-WiBS, with a lithium-metal foil pre-coated with the same LiTFSI-HFE gel as the reference electrode. All CVs were obtained at the scanning rate of 0.5 mV/s. Insets are schematic illustrations for the cell configurations used in anode and cathode CVs, respectively.

(B) Charge and discharge voltage profiles of graphite electrode pre-coated with LiTFSI-HFE gel. Galvanostatic cycling was conducted in gel-WiBS using an Ag/AgCl reference electrode at 0.1 C. The counter electrode is activated carbon. The potential has been converted to a Li/Li^+ reference for convenience.

cathodic scan at ~0.70 V, which could be caused by SEI formation from mixed reductions of HFE, LiTFSI, and trace residual of DMC, but it disappears in the following scans, reminiscent of the irreversible process associated with the interphase formation.[2] At the end of this formation process, the majority of the LiTFSI-HFE gel should have been consumed, and a solid interphase should now exist on the graphite surface that should imitate a composite interphase with mixed characteristics of inorganic/organic traits, similar to the SEI formed in non-aqueous electrolytes. The sharp and symmetric cathodic/anodic peaks demonstrate the excellent kinetics of Li^+-intercalation chemistry. Also displayed in Figure 2A is CV performed on a cathode material $LiVPO_4F$ in gel-WiBS, whose delithiation reaction occurs at ~4.20 V. The coupling of graphite and $LiVPO_4F$ in gel-WiBS would create a 4.0 V aqueous LIB. It should be pointed out that the counter electrode for the cathode CV is actually a Li-metal foil also pre-coated with LiTFSI-HFE gel, which protected it in gel-WiBS. This fact alone showcases the robust interphase formed from the HFE-based additive.

More rigorous tests on the reliability of such a new interphase were conducted in a galvanostatic manner, where the protected graphite electrode was repeatedly lithiated and delithiated at constant current (Figure 2B). The voltage profiles clearly reveal that lithiated graphite compound (LIC) is successfully formed at stage 1, as demonstrated by the plateau at <0.20 V as well as the specific capacity of ~325 mAh/g obtained. The Coulombic efficiency (CE%) in the first cycle is ~85%, which is slightly lower than the first cycle CE% (88%) of the same graphite anode in a typical non-aqueous electrolyte, 1.2 M lithium hexafluorophosphate in ethylene carbonate and ethyl methyl carbonate at 30:70 weight ratio ($LiPF_6$/EC/EMC 30:70; Figure S8, denoted as Gen II hereafter). The corresponding irreversible capacity should account for the formation of interphase from the reduction of LiTFSI-HFE. The effectiveness of such interphase is immediately reflected in the CE% of the following cycles, which rapidly rise to 99.3% for the second cycle and approaches 99.5% for the later cycles.

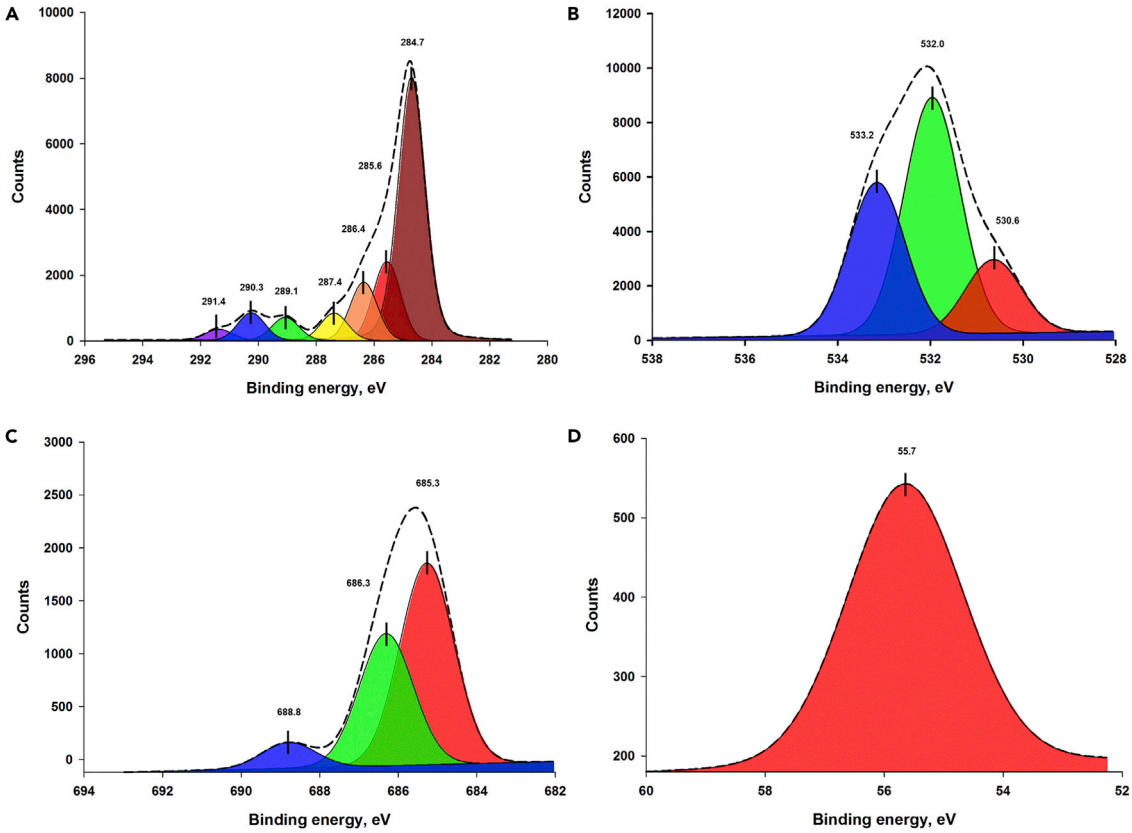

Figure 3. Chemical Analysis of Graphite Anode Surface

(A–D) XPS spectra of C 1s (A), O1s (B), F 1s (C), and Li 1s (D) on graphite electrodes recovered from cells that were cycled for a few times before being delithiated.

The chemical composition of the interphase on cycled graphite was analyzed using X-ray photoelectron spectra (XPS). The graphite electrodes were recovered from the cycled cells at both lithiated and delithiated states, and were first washed with HFE and then DMC to remove residual HFE and LiTFSI, while the subsequent high vacuum prior to XPS sample entry should have removed any trace residual HFE, considering that the boiling temperature of HFE is merely 93°C. We noticed that, due to the high reactivity of the lithiated graphite (LiC_6), there seems to be reaction between LiC_6 and the rinsing solvent DMC when the LiC_6 electrode was immersed into the latter. Such reaction produces interphase artifacts, as demonstrated by the unusually high abundance of carbonate species at 289 eV (Figure S9), which is typical for alkyl-carbonates as reduction products from carbonate solvents such as DMC. Therefore, we only adopted the data collected from the delithiated graphite (Figure 3). XPS C 1s spectra (Figure 3A) strongly suggest that HFE indeed has been reductively decomposed to form an interphase on graphite, as demonstrated by the ethereal carbon species at high abundances (~286 eV), as well as the presence of C-F at 291.4 eV. The latter could also arise from the products generated by the reductive decompositions of TFSI, as described previously.[6] O 1s and F 1s spectra separately provide strong evidence for the reductive decomposition of both HFE and TFSI (Figures 3B and 3C), with the presence of SO_2 (533.2 eV) and CF_2-O (537 eV) species in the former, and C-F (686.3 eV) and C-F_3 (688.8 eV) in the latter. Inorganic species LiF was also detected as an interphase ingredient, supported by 685.3 eV in F 1s (Figures 3C) and 55.7 eV in Li 1s (Figure 3D) spectra, respectively. Thus, this composite

interphase would consist of a mixture of organic fluorinated hydrocarbon and inorganic fluorides, both of which have been found previously in interphases formed from diversified non-aqueous electrolytes. One interesting feature is perhaps the likelihood of carbonate (CO_3^{2-}) species, as demonstrated by 289–290 eV signals in C 1s and 532 eV signals in O 1s. The origin of carbonate-like species might be the trace residual of DMC in the LiTFSI-HFE gel, or the CO_2 dissolved in WiBS, as the preparation of this aqueous electrolyte and its gel was conducted in an ambient environment.

The cycled graphite electrodes were also examined under transmission electron microscope (TEM), which reveals an amorphous thin layer less than 10 nm in thickness covering the crystalline graphite (Figure S10), in sharp contrast with the *ad hoc* interphases formed by reduction of TFSI in WiSE,[6] WiBS,[11] or the sodium version of WiSE,[10] where all the interphases seemed to be perfectly crystalline with LiF or NaF as the main component. We attributed this distinct difference to the participation of HFE, whose reductive decomposition into fluorine-containing hydrocarbon oligomers or polymers should be responsible for bringing amorphous and organic characteristics into the interphase, thus rendering the interphase more similar to the SEIs formed in non-aqueous electrolytes.

Having confirmed the formation of a new interphase from LiTFSI-HFE and its effectiveness in stabilizing graphite and even Li metal in WiBS, we now can couple such protected anode materials with different cathode chemistries. As described previously,[4] the redox potentials of most cathode materials ($LiMnO_2$,[6,9] $LiCoO_2$,[9,13] etc.) reside comfortably below the anodic stability limit of either WiSE and WiBS, granting us the "anodic amenity" in sharp contrast to a "cathodic challenge." A series of 4.0 V class aqueous Li-ion full cells were thus assembled, using $LiVPO_4F$ or $LiMn_2O_4$ versus either graphite or Li metal, where the whole anode side (composite as well as substrate) was pre-coated with a thin layer of LiTFSI-HFE gel, and gel-WiBS was used as the bulk electrolyte. Figure 4 demonstrates the cycling stabilities of such cells at room temperature (~25°C). All these full aqueous LIBs operate reversibly at or above 4.0 V plateaus for up to 50 cycles, delivering capacities close to the corresponding theoretical values. Adding 1% fluoroethylene carbonate (FEC) to the HFE gel results in better cycling performance (~70 cycles Figure S11), indicating that the quality of the SEI formed is quite sensitive to the chemical composition of the precoated interphase precursor and should see much improvement in the future. Preliminary tests at elevated temperature (55°C) (Figure S12) showed faster fading rate in capacity; however, decent cell operation continued without immediate and sudden failure, demonstrating that the aqueous SEI formed, although not ideal, is indeed robust.

Although the reversibility of the above cells is still less than ideal, as demonstrated by gradually fading capacities and an average CE% between 98% and 99.5%, the fact that these anode materials can be reversibly cycled in aqueous electrolytes based on gel-WiSE represents a fundamental breakthrough itself. It enables a quantum leap in the energy density of aqueous batteries and marks the elimination of the clear demarcation drawn between aqueous and non-aqueous batteries by their respective energy output.

DISCUSSION

The safety of these 4.0 V class aqueous Li-ion cells would be ensured by the non-flammable nature of aqueous electrolyte, as well as the low reactivity of WiSE or

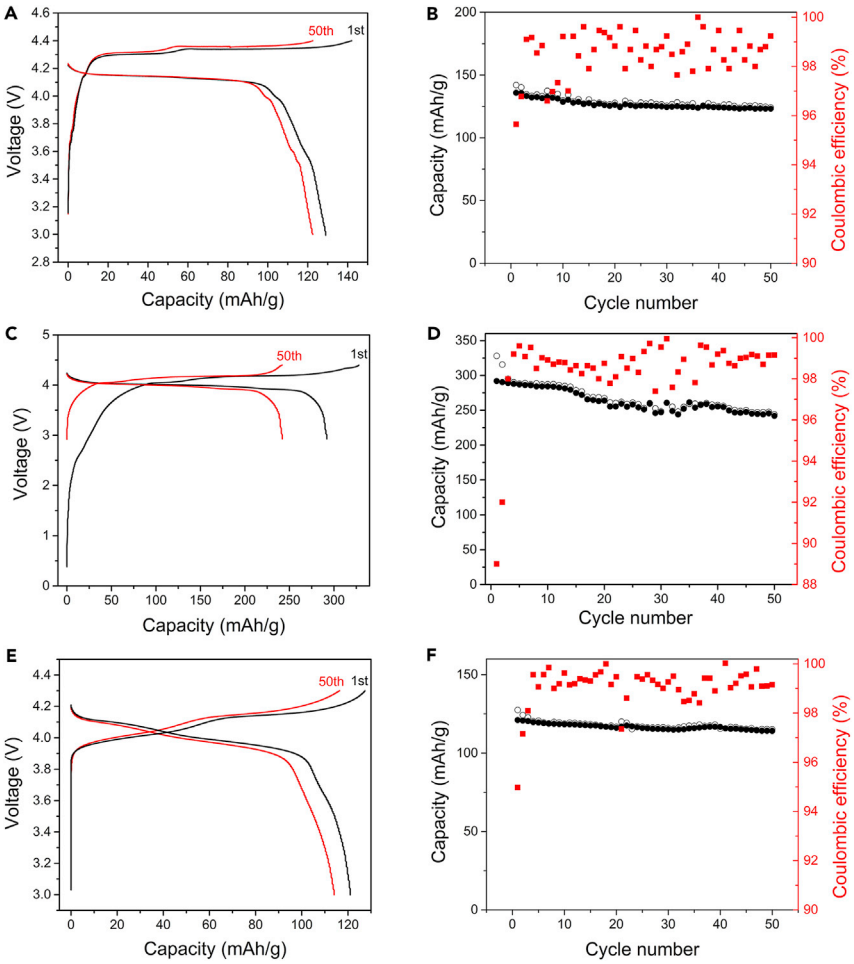

Figure 4. The Charge and Discharge Voltage Profiles and Cycle Performances of Various 4.0 V Class Aqueous Li-Ion Batteries

(A and B) The voltage profile (A) and cycling stability (B) of $LiVPO_4F$ versus Li metal at 0.3 C. The capacity is based on cathode mass.

(C and D) The voltage profile (C) and cycling stability (D) of $LiVPO_4F$ versus graphite at 0.3 C. The capacity is based on anode mass.

(E and F) The voltage profile (E) and cycling stability (F) of $LiMn_2O_4$ versus Li metal at 0.3 C. The capacity is based on cathode mass.

its gels toward Li metal (Figures S1 and S2; Movies S1 and S2). The LiTFSI-HFE gel shows similar inertness toward Li metal (Figure S6). Hence, even if the interphase formed from LiTFSI-HFE ruptures for any reason, such slow reactions between lithiated graphite (or Li metal) with gel-WiSE would still help prevent a catastrophic ending of the cells. This "gracious failure" significantly differentiates these 4.0 V aqueous Li-ion cells from the cells using Li metal protected by dense ceramic solid electrolyte in dilute aqueous electrolytes, where any crack or defect in the ceramic electrolyte layer results in a vehement reaction between Li metal and water. Additional safety validation on the material level comes from the thermal stability of the electrolyte itself as well as its chemical stability with the charged electrodes, both of which were evaluated with differential scanning calorimetry (DSC). To ensure reproducibility, at least two scans were conducted for each sample. Figure S13 compares the vapor pressure of both WiBS and Gen II as measured in a special pre-perforated DSC pan. While Gen II shows onset of evaporation of the bulk electrolyte at

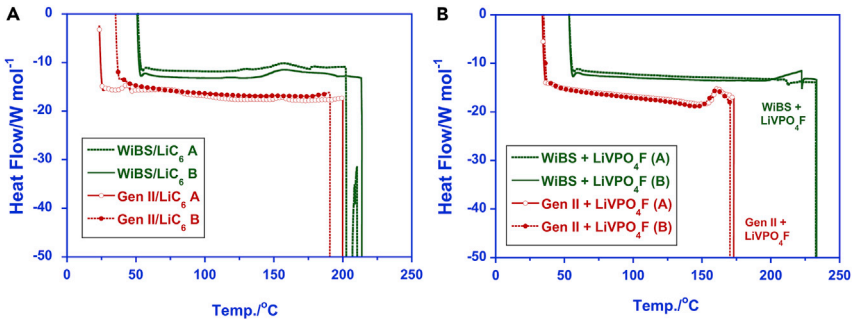

Figure 5. Thermal Stability of Aqueous Electrolyte in Presence of Charged Anode and Cathode Materials

(A and B) DSC scans of lithiated graphite (LiC_6) electrodes (A) and delithiated $LiVPO_4F$ (B) in presence of gel-WiBS and $LiPF_6$/EC/EMC 30:70, respectively.

~110°C because of EMC (boiling point 110°C), the escape of water from WiBS is much more difficult, indicating that water molecules have been tightly bound by the high ion population. These electrolytes were also loaded into hermetical DSC pans, and the rupture temperature was used as the indicator of thermal inertness (Figure S14). Again, WiBS showed higher thermal stability by remaining inactive until ~220°C before the pressure of the steam ruptured the pans, while the pans containing Gen II opened much earlier between 160°C and 180°C. More important is the chemical reactivity demonstrated by these electrolytes in the presence of charged electrodes, i.e., lithiated graphite LiC_6 and delithiated cathode $LiVPO_4F$. These electrodes were recovered from the full aqueous Li-ion cells at 100% charged state (4.3 V) and then sealed into hermetic pans with ~10 mg WiBS or Gen II. While WiSB/LiC_6 displayed similar (but slightly lower) reactivity than Gen II/LiC_6 (Figure 5A), significant difference exists between the two cathode/electrolyte combinations; WiSB/$LiVPO_4F$ is much more stable than Gen II/$LiVPO_4F$ by rupturing at a temperature >50°C higher (Figure 5B). According to previous safety investigations of LIBs, the major heat generated during the thermal runaway is attributed to the reaction between delithiated cathode and electrolyte, while the reaction between lithiated anode and electrolyte generates much less heat but often serves as a trigger to the self-propagating reactions.[14] As the fuel in the chemical combustion, non-aqueous electrolyte is often a key factor responsible for catastrophic cell failures. The above DSC results seem to suggest that the replacement of non-aqueous electrolytes by an aqueous counterpart renders the 4.0 V aqueous Li-ion cell safer, although more thorough investigation is needed before definite conclusions are drawn.

The safety of these 4.0 V aqueous Li-ion cells was further validated by physical abuse of a small pouch cell constructed with the identical chemistry shown in Figure 4A, i.e., a graphite anode protected by LiTFSI-HFE gel, a $LiVPO_4F$ cathode, and WiBS. This cell of ~13.98 mAh was charged at 0.2 C until 100% state of charge (Figure S15), and then a nail was driven through it multiple times (Movie S3). No fire or smoke ensued. Surprisingly, as the multimeter in the video shows, the cell managed to maintain its open circuit voltage (OCV) at 4.03 V, which gradually decayed to ca. 0.031 V overnight (Figure S16). This is in sharp contrast to any LIB based on non-aqueous electrolytes, which would instantly short-circuit upon nail penetration as demonstrated by the drop in OCV within seconds. We attributed this sluggishness to the viscous LiTFSI-HFE gel and the conformal interphase formed after its reductive decomposition, which might partially insulate the contacts between cathode and anode at the point of puncture, and allowed the energy to dissipate at a very

sluggish pace. The detailed mechanism merits further investigation; however, this "gracious manner" of failure for a 4.0 V class Li-ion cell confirmed again the safety of the aqueous electrolytes and the success of the inhomogeneous additive strategy.

In summary, we successfully resolved the "cathodic challenge" of aqueous electrolytes by designing a unique inhomogeneous electrolyte additive approach to minimize competitive water reduction on graphite or Li-metal surfaces during the interphase formation. Upon reductive decomposition during the first charging process, the highly fluorinated additive forms a protective interphase that enables the reversible cycling of both graphite and Li-metal anodes in aqueous electrolytes. Surface analyses using XPS and TEM confirm that such interphase is of amorphous nature and consists of fluorinated hydrocarbon species along with inorganic fluoride LiF. Coupling these anode materials thus protected with various cathode chemistries leads to a series of 4.0 V class aqueous Li-ion batteries, whose energy densities approach those state-of-the-art LIBs but with significantly enhanced safety. Although the cycling stability of such 4.0 V class aqueous Li-ion batteries needs further improvement, their emergence represents a fundamental breakthrough across the gap separating aqueous and non-aqueous batteries. With further perfection of the interphase chemistry, aqueous LIBs of energy density and reversibility comparable with state-of-the-art LIBs, but without the safety concerns of the latter, will become a reality.

EXPERIMENTAL PROCEDURES

Synthesis of the WiSE and HFE/DMC Gel Electrolytes

The WiSE was prepared by dissolving 21 mol kg^{-1} LiTFSI (~98%, TCI Co., Ltd.) in water (HPLC grade), to which an additional 7 mol kg^{-1} LiOTf (~99.996%, Sigma-Aldrich) was added to make the WiBS electrolyte. Aqueous gel electrolytes (gel-WiBS) were prepared by adding 10 wt % PVA (Sigma-Aldrich) in WiBS and heated at 95°C for 5 hr under vigorous stirring. The mixture of 1,1,2,2-tetrafluoroethyl-2′,2′,2′-trifluoroethyl ether (Daikin America or Apollo) with LiTFSI (denoted as LiTFSI-HFE gel) was prepared by adding 0.5 M LiTFSI and 10 wt % PEO (Sigma-Aldrich) in HFE/DMC (volume ratio = 95:5) and heated at 70°C for 20 min under stirring.

Synthesis of the Graphite, $LiVPO_4F$, and $LiMn_2O_4$ Electrodes

The graphite anode electrodes were coated on Cu foil with a weight ratio of 90% of graphite (KS44) and 10% polyvinylidene fluoride binder (PVDF). The $LiVPO_4F$ and $LiMn_2O_4$ cathode electrodes were coated on Al foil with a weight ratio of 80% of active materials, 10% carbon black, and 10% PVDF.

Electrochemical Measurements

The three-electrode CV test of graphite and moisture-content measurements were performed in glass-bottle-like cells. The graphite electrode was pre-coated with an HFE gel layer and then immersed into gel-WiBS. The counter electrode ($LiVPO_4F$ or active carbon) and Ag/AgCl reference electrode were positioned in gel-WiBS. CV was carried out using a CHI 600E electrochemical work station. The two-electrode test cells were assembled as Swagelok cells using either $LiVPO_4F$ or $LiMn_2O_4$ as cathode, graphite or Li metal as anode, and gel-WiBS sandwiched in between as electrolyte in the absence of a separator. Before assembly, the whole anode side, which includes both active material (graphite) and current collector, was coated with LiTFSI-HFE gel, so that WiBS did not contact any part of anode directly. The cells were cycled galvanostatically on a Land BT2000 battery test system (Wuhan, China)

at room temperature. To measure the moisture content, HFE gel was exposed to WiSE at equilibrium as shown in Figure S5, then a certain amount of HFE gel was taken out and diluted with tetrahydrofuran at regular intervals for moisture-content evaluation using a Coulometer (Metrohm 899).

Other Characterizations

More details of the characterization methods followed, molecular dynamics (MD) simulation methodology, and DFT calculations are provided in Supplemental Information.

SUPPLEMENTAL INFORMATION

Supplemental Information includes Supplemental Experimental Procedures, 16 figures, and 3 movies and can be found with this article online at http://dx.doi.org/10.1016/j.joule.2017.08.009.

AUTHOR CONTRIBUTIONS

C.Y., C.W., and K.X. conceived the idea and co-wrote the manuscript. C.Y., J.C, T.Q., A.v.C., and N.E. carried out the synthesis, material characterizations, and electrochemical evaluation. J.V. and O.B. conducted MD simulations and QC calculations. X.F., W.S., M.S.D., and M.A.S. assisted with the material characterizations.

ACKNOWLEDGMENT

The principal investigators (C.W. and K.X.) received the financial support from the US Department of Energy ARPA-E Grant DEAR0000389. J.V. and M.S. were supported by the Oak Ridge Associated Universities (ORAU) Postdoctoral Fellowships W911NF-16-2-0107 and W911NF-16-2-0187.

Received: June 11, 2017
Revised: July 21, 2017
Accepted: August 11, 2017
Published: September 6, 2017

REFERENCES

1. Hammami, A., Raymond, N., and Armand, M. (2003). Lithium-ion batteries: runaway risk of forming toxic compounds. Nature *424*, 635–636.

2. Xu, K. (2004). Nonaqueous liquid electrolytes for lithium-based rechargeable batteries. Chem. Rev. *104*, 4303–4417.

3. O'M Bockris, J., and Reddy, A.K.N. (2000). Modern Electrochemistry, *Vol. 2*, Second Edition (Plenum Press).

4. Xu, K., and Wang, C. (2016). Batteries: widening voltage windows. Nat. Energy *1*, 16161.

5. Kim, H., Hong, J., Park, K.-Y., Kim, H., Kim, S.-W., and Kang, K. (2014). Aqueous rechargeable Li and Na ion batteries. Chem. Rev. *114*, 11788–11827.

6. Suo, L., Borodin, O., Gao, T., Olguin, M., Ho, J., Fan, X., Luo, C., Wang, C., and Xu, K. (2015). "Water-in-salt" electrolyte enables high-voltage aqueous lithium-ion chemistries. Science *350*, 938–943.

7. Yamada, Y., Usui, K., Sodeyama, K., Ko, S., Tateyama, Y., and Yamada, A. (2016). Hydrate-melt electrolytes for high-energy-density aqueous batteries. Nat. Energy *1*, 16129.

8. Zhao, J., Li, Y., Peng, X., Dong, S., Ma, J., Cui, G., and Chen, L. (2016). High-voltage Zn/LiMn0.8Fe0.2PO4 aqueous rechargeable battery by virtue of "water-in-salt" electrolyte. Electrochem. Commun. *69*, 6–10.

9. Yang, C., Suo, L., Borodin, O., Wang, F., Sun, W., Gao, T., Fan, X., Ma, Z., Amine, K., Xu, K., and Wang, C. (2017). Unique aqueous Li-ion/sulfur chemistry with high energy density and reversibility. Proc. Natl. Acad. Sci. USA *114*, 6197–6202.

10. Suo, L., Borodin, O., Wang, Y., Rong, X., Sun, W., Fan, X., Xu, S., Schroeder, M.A., Cresce, A., Wang, F., et al. (2017). "Water-in-salt" electrolyte makes aqueous sodium-ion battery safe, green, and long-lasting. Adv. Energy Mater. http://dx.doi.org/10.1002/aenm.201701189.

11. Suo, L., Borodin, O., Sun, W., Fan, X., Yang, C., Wang, F., Gao, T., Ma, Z., Schroeder, M., Cresce, A., et al. (2016). Advanced high-voltage aqueous lithium-ion battery enabled by "Water-in-Bisalt" electrolyte. Angew. Chem. Int. Ed. *128*, 7136–7141.

12. Xu, K. (2014). Electrolytes and interphases in Li-ion batteries and beyond. Chem. Rev. *114*, 11503–11618.

13. Wang, F., Lin, Y., Suo, L., Fan, X., Gao, T., Yang, C., Han, F., Qi, Y., Xu, K., and Wang, C. (2016). Stabilizing high voltage LiCoO2 cathode in aqueous electrolyte with interphase-forming additive. Energy Environ. Sci. *9*, 3666–3673.

14. Maleki, H., Deng, G., Anani, A., and Howard, J. (1999). Thermal stability studies of Li-ion cells and components. J. Electrochem. Soc. *146*, 3224–3229.

JOUL, Volume *1*

Supplemental Information

4.0 V Aqueous Li-Ion Batteries

Chongyin Yang, Ji Chen, Tingting Qing, Xiulin Fan, Wei Sun, Arthur von Cresce, Michael S. Ding, Oleg Borodin, Jenel Vatamanu, Marshall A. Schroeder, Nico Eidson, Chunsheng Wang, and Kang Xu

Supporting Information

Methods

X-ray photoelectron spectroscopy (XPS) was performed on a PHI Versaprobe 3 instrument with a monochromated Al Kα source that produces radiation $h\nu$ = 1486 eV. The analyzed area of the sample was 100 μm × 100 μm. High resolution scans of Li 1s, C 1s, O 1s, and F1s regions were collected with a constant pass energy of 55.0 eV and a dwell step time of 100 ms while under charge neutralization to reduce differential charging. Sample spectra were calibrated to the C 1s signal for C-C occurring at 284.8 eV. Raw data curve fitting and deconvolution was performed using the Multipak software package. Curves were fit using a Shirley-type background, and symmetrical peaks of 90-100% Gaussian character. Full width half maximum (FWHM) was fixed for all deconvoluted peaks within each high resolution element scan.

Thermal scans for chemical stability and vapor pressure were performed using a differential scanning calorimeter (DSC) by TA Instruments, Model MDSC 2920. For vapor pressure, a special aluminum sample lid (Perkin Elmer N519-0788) with a pinhole of 50 μm diameter replaced the usual lid, and calibration was done with the boiling points of water (100 °C) and n-decane (174.15°C). For chemical stability, aluminum sample pan and lid (Perkin Elmer 2190062) were used to hermetically seal about 10 mg of electrolyte and a small piece of an electrode on a substrate, using a Perkin Elmer crimper 2190061. These samples were left at either room temperature or 50 °C for at least 15 hours for proper wetting of the enclosed electrode materials before they were heated up on the DSC at the rate of 5 °C/min until the sample burst, which occurs nominally at around 2 atm. Calibration for this part of the experiment was done with the melting points of cyclohexane (6.54 °C), indium (156.6°C), and tin (231.88 °C).

In order to provide insight into the interfacial structure of WiBS electrolyte at graphite electrodes, a number molecular dynamics (MD) simulations were performed on 21 m LiTFSI + 7 m LiOTF aqueous solution at 363 K. Higher temperature was chosen to facilitate equilibration of the interfacial structure on the simulation timescale. The simulation cell was comprised of 192 LiTFSI , 64 LiOTF, and 512 water molecules that were confined between two graphite electrodes with their basal plane in contact with electrolyte similar to our previous work on aprotic

electrolytes.[1] MD simulations were performed utilizing a modified version of the CHARMM polarizable force field [2] for H_2O in conjunction with the APPLE&P many-body polarizable force field parameters for ions/ion and ion/water interactions.[3,4] Functional form of APPL&P force field is discussed in details elsewhere.[5]

A constant potential methodology that accounts for the electrode polarization by ions and solvent from electrolyte was used. [6,7] While a number of voltages from 0 V to 5 V was applied between two graphite electrodes, we focus our analysis on the negative electrode with potentials of -2.5 V and -0. 5 V vs. bulk electrolyte after a potential of zero charge (PZC= -0.57 V) was subtracted. Assuming that PZC is close to the experimentally measured open circuit voltage of 3 V vs. Li/Li^+, these potentials correspond to 0.5 V and 2.5 vs. Li/Li^+. The short range interactions such as repulsion and dispersion were truncated beyond 12 Å, while the reciprocal part of smooth particle mesh Ewald (SPME) [8] was calculated in two dimensions. [9,10] A Nose Hoover [11] chain thermostat was used to control temperature.

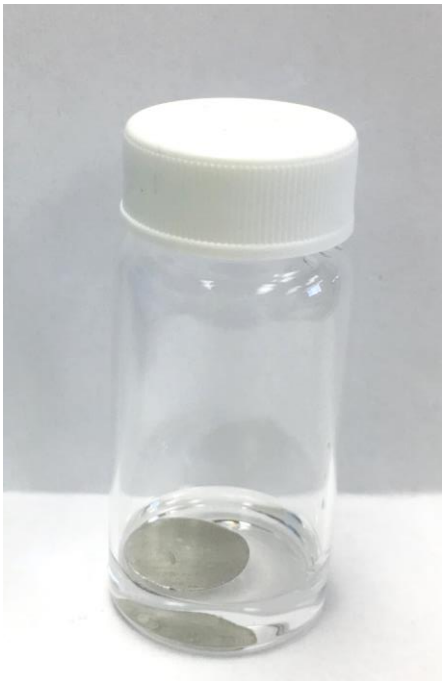

Figure S1. The slow reactivity between Li metal and WiBS (21 m LiTFSI+ 7 m LiOTf in water).

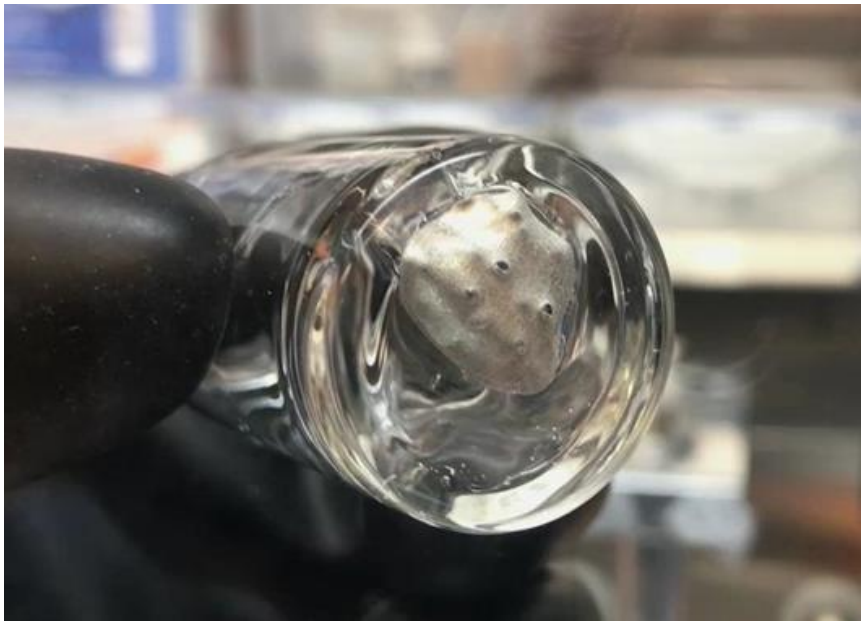

Figure S2. The stability between Li metal and WiBS gel.

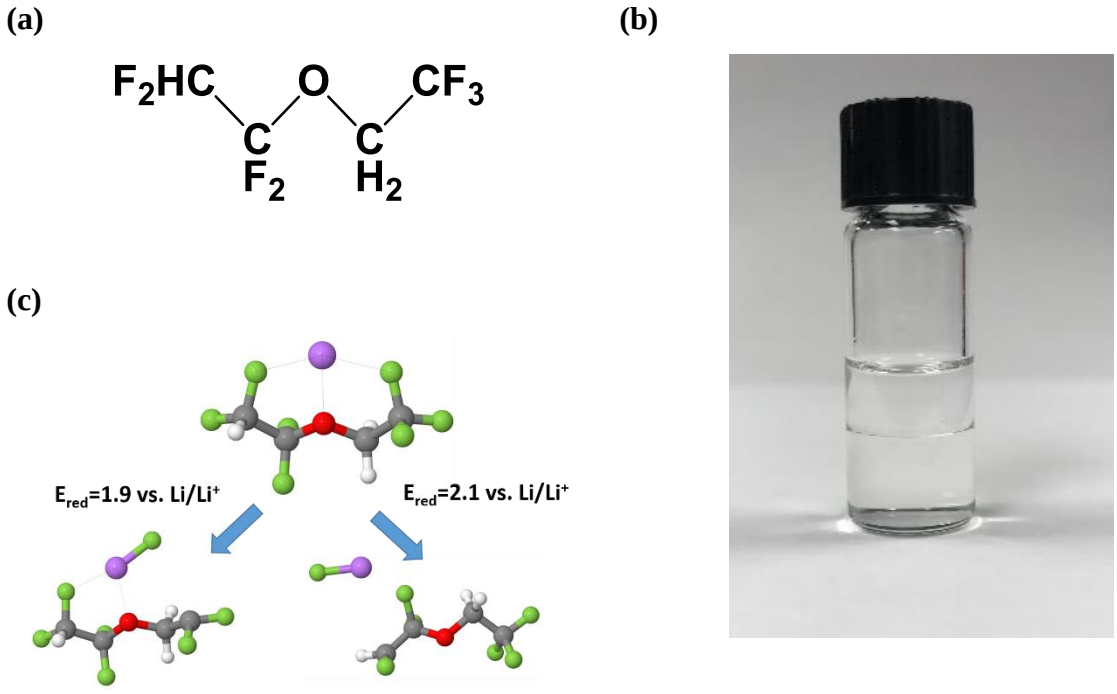

Figure S3. (a) The molecular structure of HFE (1,1,2,2-tetrafluoroethyl-2',2',2'-trifluoroethyl ether); (b) The immiscibility between HFE additive (upper phase) and WiBS electrolyte (lower phase); (c) Reduction potentials of Li-HFE from M05-2X/6-31+G(d,p) density functional theory (DFT) calculations with SMD(e=20) solvation model using previously described methodology.[12] Similar reduction potentials were predicted for the Li-FEC complexes.

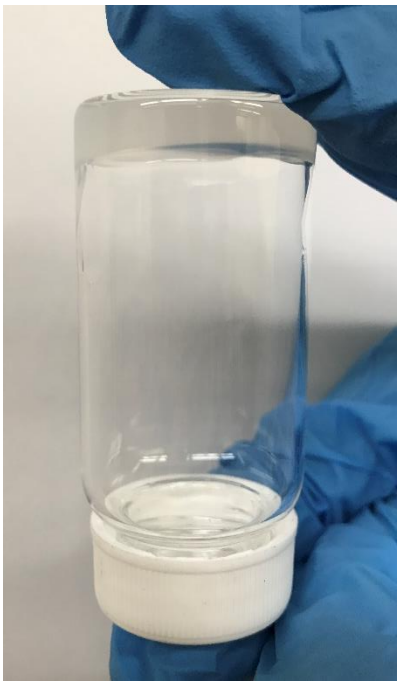

Figure S4. The translucent LiTFSI-HFE gel.

Figure S5. The immiscibility between LiTFSI-HFE gel and WiBS.

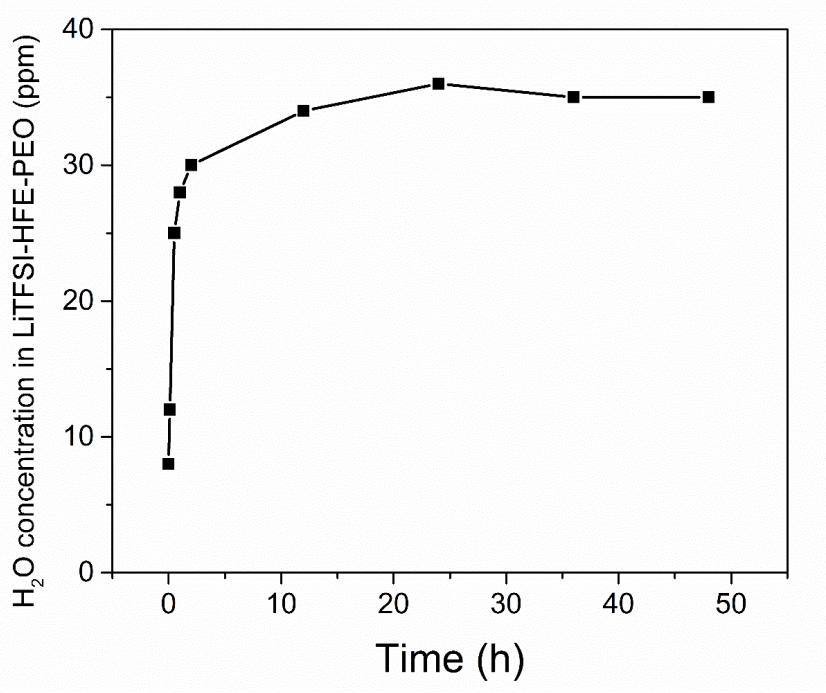

Figure S6. The time-dependence of moisture-content in LiTFSI-HFE gel with exposure to WiBS GPE.

Figure S7. The stability between Li metal and LiTFSI-HFE gel.

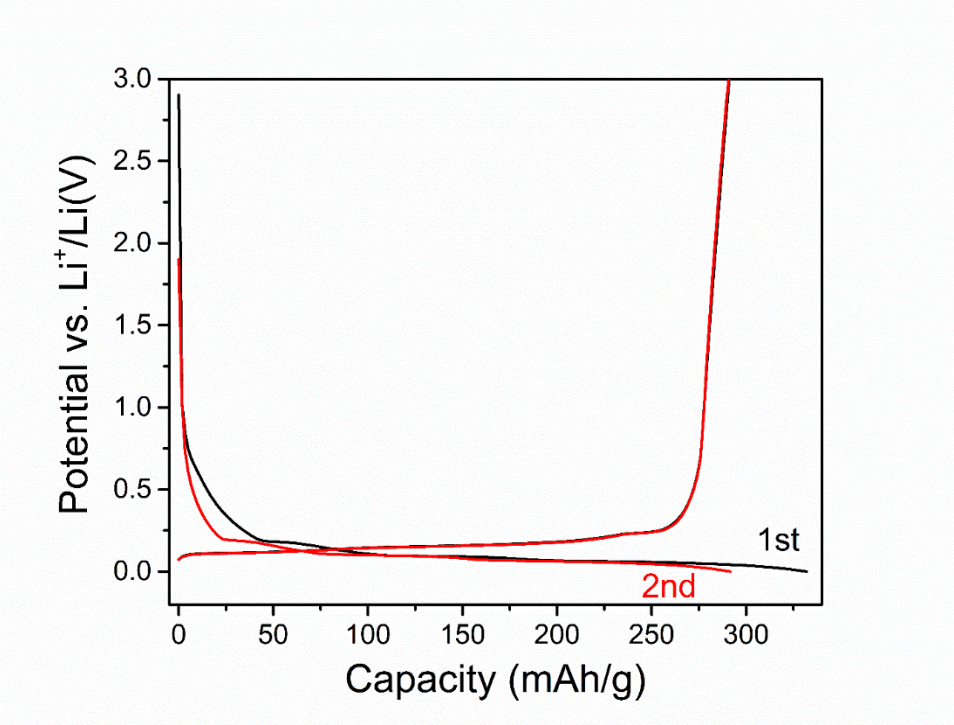

Figure S8 Charge and discharge voltage profiles of graphite electrode in Gen II non-aqueous electrolyte 1.2 m $LiPF_6$/EC/EMC (30:70).

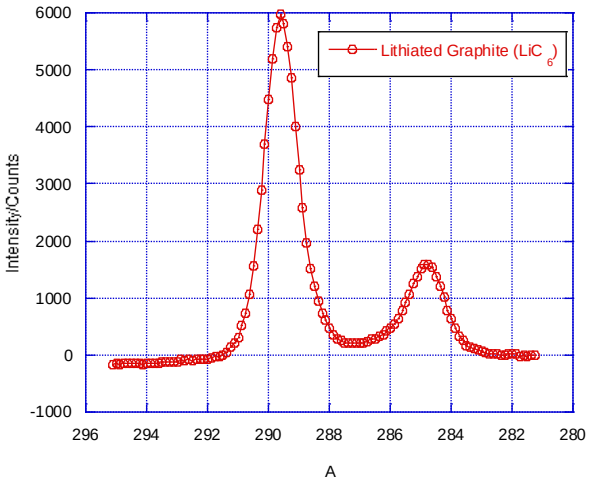

Figure S9 Artifact carbonate species (289 eV) in high abundance generated by reaction between lithiated graphite and rinsing solvent DMC.

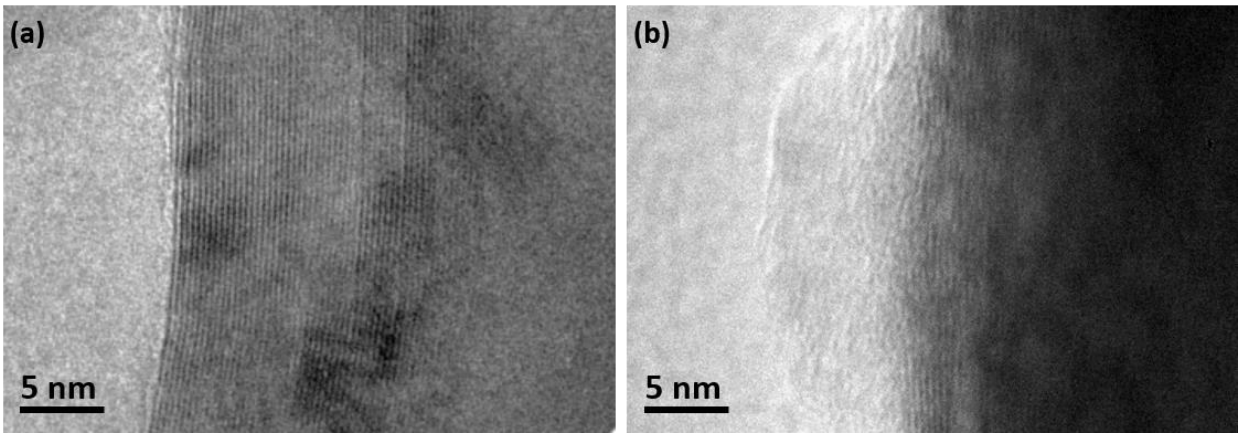

Figure. S10 High-resolution TEM images of graphite (a) before and (b) after 20 cycles LiTFSI-HFE at 0.2 C.

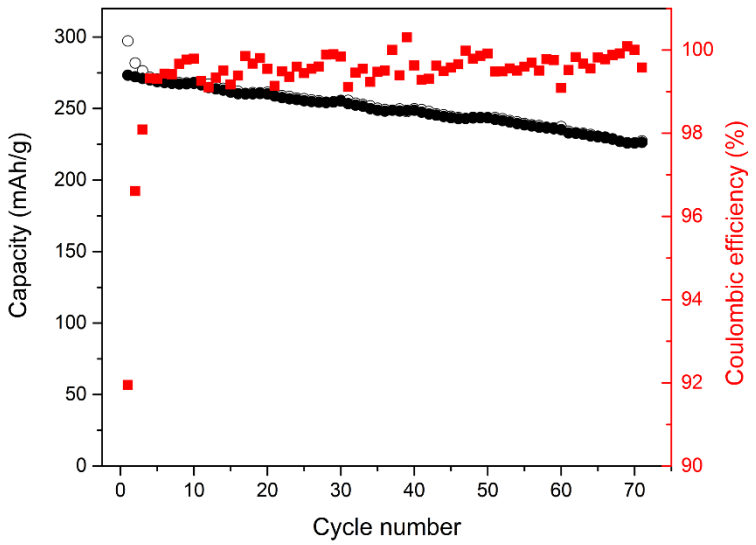

Figure. S11 Cycling performances of full aqueous Li-ion cell based on graphite/$LiVPO_4F$ at 0.3 C. The pre-coated SEI precursor consists of 0.5 M LiTFSI and 10 wt.% PEO in the HFE/DMC/FEC (Volume ratio = 95:4:1). The capacity is based on anode material mass.

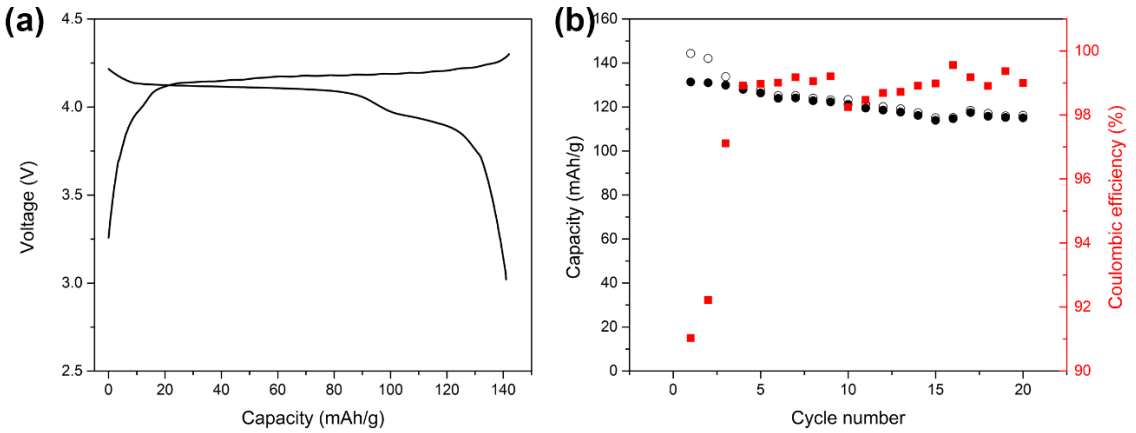

Figure S12. (a) The cycling voltage profiles and (b) cycling stability of cathode half cell Li/LiVPO$_4$F at 0.3 C and 55 ^{o}C. The capacity is based on cathode material mass.

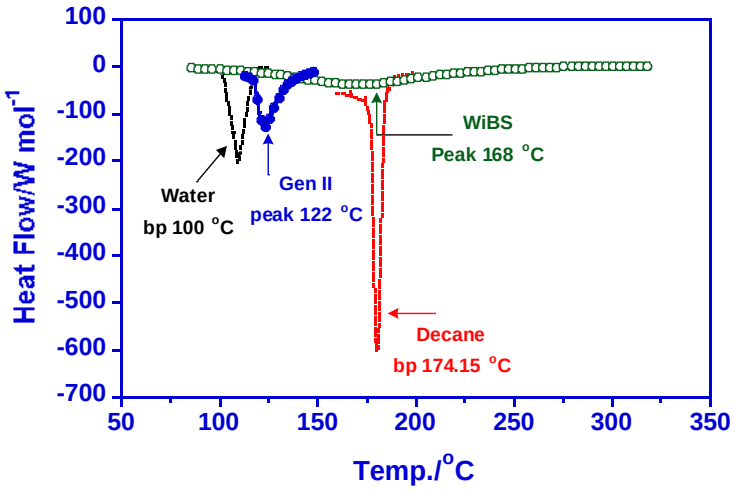

Figure. S13 Comparison of vapor pressure for Gen II electrolyte (1.2 M LiPF$_6$/EC/EMC 30:70) and WiBS in perforated DSC pans. Water and decane were used therein as reference.

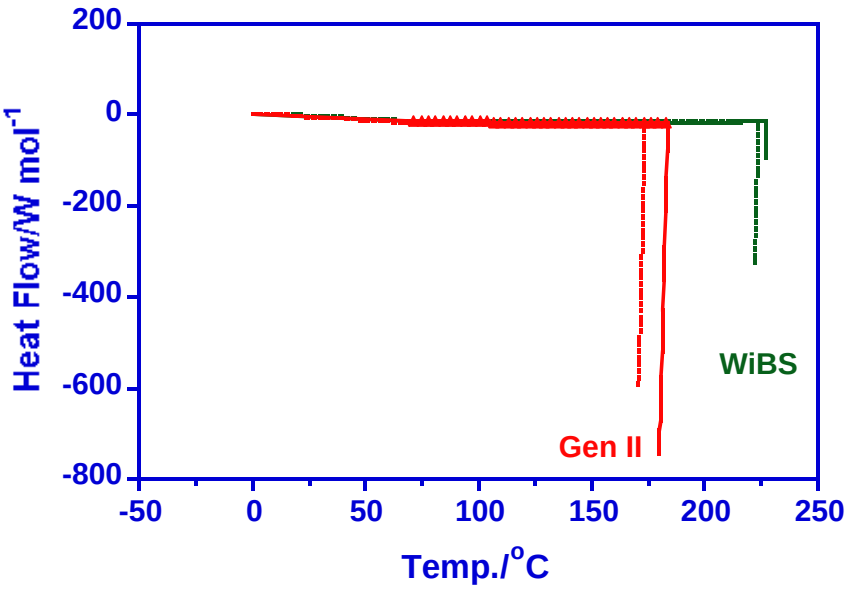

Figure. S14 Comparison of Gen II electrolyte (1.2 M LiPF6/EC/EMC 30:70) and WiBS using hermetically sealed DSC pans. Two separate scans were collected from each electrolyte to confirm the reproducibility.

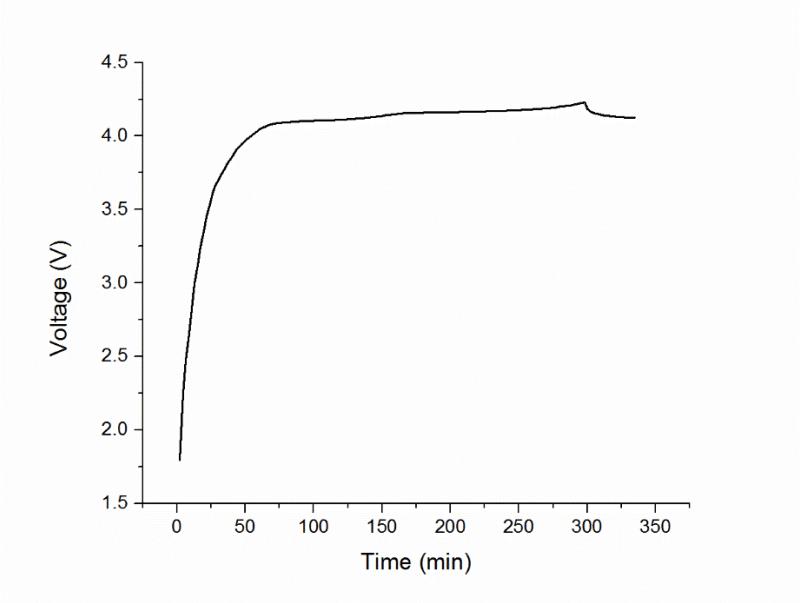

Figure. S15 Charging profile of a full aqueous Li-ion pouch cell constructed with graphite/WiBS/$LiVPO_4F$. The cell capacity is ~13.9 mAh, and the cell was charged at 0.2 C (2.8 mA) before being punctured with a nail (see Video 3).

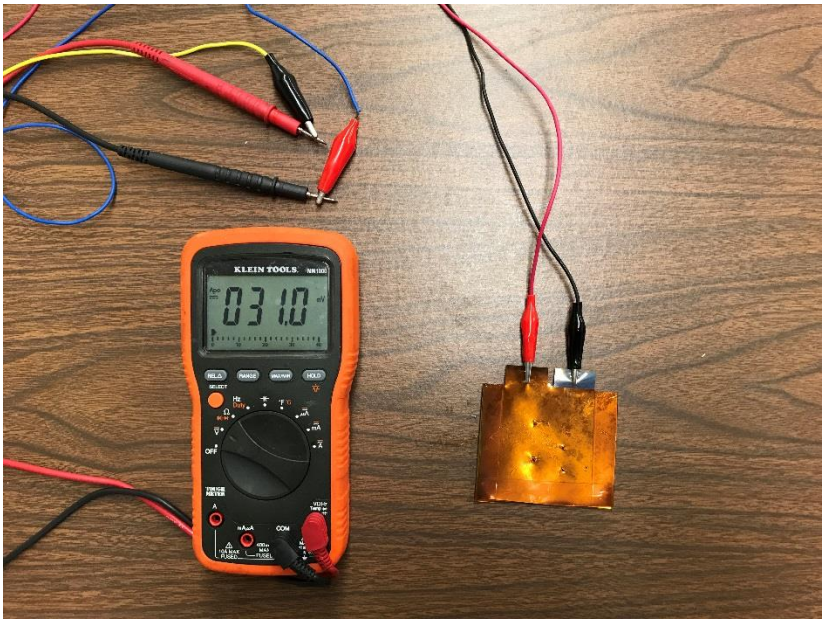

Figure. S16 The above full aqueous Li-ion cell after being punctured with nail in Video 3. The OCV gradually decays to 31 mV after 24 hours.

Reference

1 Vatamanu, J., Borodin, O. & Smith, G. D. Molecular Dynamics Simulation Studies of the Structure of a Mixed Carbonate/$LiPF_6$ Electrolyte near Graphite Surface as a Function of Electrode Potential. *J. Phys. Chem. C* **116**, 1114-1121, doi:10.1021/jp2101539 (2012).

2 Starovoytov, O. N., Borodin, O., Bedrov, D. & Smith, G. D. Development of a Polarizable Force Field for Molecular Dynamics Simulations of Poly (Ethylene Oxide) in Aqueous Solution. *J. Chem. Theory Comput.* **7**, 1902-1915, doi:10.1021/ct200064u (2011).

3 Suo, L. *et al.* Advanced High-Voltage Aqueous Lithium-Ion Battery Enabled by "Water-in-Bisalt" Electrolyte. *Angewandte Chemie International Edition* **55**, 7136-7141, doi:10.1002/anie.201602397 (2016).

4 Suo, L. *et al.* "Water-in-salt" electrolyte enables high-voltage aqueous lithium-ion chemistries. *Science* **350**, 938-943, doi:10.1126/science.aab1595 (2015).

5 Borodin, O. Polarizable Force Field Development and Molecular Dynamics Simulations of Ionic Liquids. *J. Phys. Chem. B* **113**, 11463-11478, doi:10.1021/jp905220k (2009).

6 Reed, S. K., Lanning, O. J. & Madden, P. A. Electrochemical interface between an ionic liquid and a model metallic electrode. *The Journal of Chemical Physics* **126**, 084704, doi:doi:http://dx.doi.org/10.1063/1.2464084 (2007).

7 Siepmann, J. I. & Sprik, M. Influence of surface topology and electrostatic potential on water/electrode systems. *The Journal of Chemical Physics* **102**, 511-524, doi:doi:http://dx.doi.org/10.1063/1.469429 (1995).

8 Essmann, U. *et al.* A smooth particle mesh Ewald method. *The Journal of Chemical Physics* **103**, 8577-8593, doi:doi:http://dx.doi.org/10.1063/1.470117 (1995).

9 Kawata, M., Mikami, M. & Nagashima, U. Computationally efficient method to calculate the Coulomb interactions in three-dimensional systems with two-dimensional periodicity. *The Journal of Chemical Physics* **116**, 3430-3448, doi:doi:http://dx.doi.org/10.1063/1.1445103 (2002).

10 Kawata, M. & Mikami, M. Rapid calculation of two-dimensional Ewald summation. *Chemical Physics Letters* **340**, 157-164, doi:http://dx.doi.org/10.1016/S0009-2614(01)00378-5 (2001).

11 Hoover, W. G. Canonical dynamics: Equilibrium phase-space distributions. *Physical Review A* **31**, 1695-1697 (1985).